# Empirical potential for the interaction between molecular hydrogen and graphite

D. Y. Sun,[1,2] J. W. Liu,[1] X. G. Gong,[3] and Zhi-Feng Liu[1,*]

[1]*Department of Chemistry and Centre for Scientific Modeling and Computation, Chinese University of Hong Kong, Shatin, Hong Kong, China*

[2]*Key Laboratory of Optical and Magnetic Resonance Spectroscopy and Department of Physics, East China Normal University, Shanghai 200062, China*

[3]*Surface Physics Laboratory and Department of Physics, Fudan University, Shanghai 200433, China*

(Received 13 October 2006; revised manuscript received 5 December 2006; published 26 February 2007)

High level *ab initio* results on the interaction between $H_2$ and graphite have recently become available, and in this paper, $H_2$-graphite potentials have been fitted to model such interactions. The popular Lennard-Jones formula is found to be inadequate, and its strong repulsive part must be replaced to fit the full range of interactions, from the long range attraction to the short range repulsion. Two isotropic empirical forms are obtained, and both produce excellent fit to the *ab initio* results and should provide good description for the interactions between hydrogen and graphitic materials, both in the physisorption and the high pressure regimes. Our calculations also show that density functional theory is inadequate to describe the $H_2$-graphite interactions in high pressure. The newly obtained exp-6-8-10 is also applied to the problem of trapping $H_2$ in graphite, and the calculated critical pressure is considerably higher than that obtained before by density functional theory calculations.

DOI: 10.1103/PhysRevB.75.075424 PACS number(s): 68.43.Bc, 62.50.+p, 61.43.Bn

## I. INTRODUCTION

The interaction between molecular hydrogen and graphite is important because it is a model for many types of interactions between hydrogen and graphitic materials. The promises of such materials for the storage of hydrogen as a clean fuel for mobile applications have aroused much interest, especially in the case of carbon nanotubes.[1–3] For physisorption based methods, the adsorption energy and equilibrium distance due to van der Waals interaction are among the crucial factors that determine the storage capacity.[4,5] The repulsive region of the van der Waals potential is also important to understand the behavior of hydrogen in high density states, either by the confinement achieved in nanocavity or by the application of high pressure.[6–9]

It is well understood that the van der Waals potential for molecular hydrogen is weak, compared to other typical gas molecules, due to the fact that there are only two electrons on $H_2$ in a compact molecular orbital produced by the linear combination of two 1*s* atomic orbitals.[10] For the interaction between hydrogen molecules, experimental data over a wide range of temperature and pressure are available for fitting an empirical potential energy surface (PES).[10,11] For the interaction between a hydrogen molecule and a solid surface such as graphite, first principles calculations are often needed. The flat and simple two-dimensional structure of graphite provides an ideal model to compute, validate and test the PES, which could then be adapted for other graphitic materials. For plane wave based density functional (DFT) theory calculations, a graphene layer is easily modeled as a two-dimensional periodic structure.[12] For Gaussian based *ab initio* calculations, a graphene layer is usually modeled in a cluster model by polycyclic aromatic hydrocarbons (PAH).[13–17]

However, it is nontrivial to get the $H_2$-graphite interaction potential right. DFT is known to be inadequate for the modeling of van der Waals interactions. Typically, the adsorption energy is overestimated and the equilibrium distance is too short for results obtained within local density approximation (LDA). On the other hand, the adsorption energy is underestimated and the distance is too long when gradient corrections are added to the functional.[18] The DFT calculation results for the $H_2$-graphite system also fit such a general pattern, for both plane wave based[12] and Gaussian based methods.[14,16] More reliable results can be obtained by *ab initio* methods, with post-Hartree-Fock treatment,[13,14,16] although a number of factors must be carefully considered and analyzed, including the size of basis sets, the size of PAH rings, basis set superposition errors (BSSE), and the methods of post-Hartree-Fock treatments for electron correlation effects.[13,14,16] After all, the adsorption energy of $H_2$ on graphite surface was estimated experimentally to be just above 50 meV,[19] which was a challenge to reproduce with *ab initio* calculations when a reasonably large PAH was used as a model for graphene. To date, the most elaborate calculations were performed at the MP2 level with a large aug-cc-pVTZ basis set, by Ferre-Vilaplana[13] and by Heine and co-workers.[14] The adsorption energy of $H_2$ on a coronene model for graphene was found to be 0.066 eV (Ref. 13) and 0.064 eV,[14] respectively, which provided a consistent *ab initio* description of the depth and shape for the physisorption well.

Another important part of the PES is in the repulsive region. In correspondence to the weak adsorption of $H_2$, its repulsive potential is also weaker than typical gases, which makes molecular hydrogen highly compressible.[10,11] For storage purpose, the properties of molecular hydrogen in high density states have aroused interests in recent studies.[6–9] Based on LDA calculations, our group identified a state of confinement at GPa pressure and low temperature (100–200 K), in which a hydrogen molecule was sandwiched between two hexagonal rings on two graphene

 

sheets.[8] More recently, van den Berg and co-workers have systematically compared DFT and force field calculations for molecular hydrogen under high pressure in nanoporous siliceous materials,[9] and found significant discrepancy between DFT and force field results.

These results raised an interesting and important question: while it is well understood that DFT is inadequate for the attractive region of the $H_2$-graphite potential, is DFT suitable for the repulsive region? It should also be noted that using a Lennard-Jones potential to describe the repulsive interactions between $H_2$ and graphite in force field calculations[9] could also be problematic, because such a potential is known to be inadequate for the experimentally measured full range of interactions between two hydrogen molecules.[10]

In recent *ab initio* studies,[13,14] the interaction energy between $H_2$ and graphite was calculated over both the attractive and repulsive regions at high accuracy with post-Hartree-Fock treatment and large basis sets. It is worthwhile to parametrize these results into an empirical formula, which should be very useful in future simulations for both the physisorption and the high density state of hydrogen. Such a PES also provides an independent check on the quality of both the DFT and force field calculations reported before.[8,9]

## II. COMPUTATIONAL DETAILS

### A. PES fitting

A $H_2$ molecule is treated as a structureless particle, and the interaction between $H_2$ and a graphene layer is modeled by the summation over $H_2$-C pair potentials. Three types of potentials are fitted and compared in our study. The simplest one is of course the Lennard-Jones (12–6 LJ) potential, which has been very popular among computational studies on the interaction between $H_2$ and carbon materials. A more complicated form is similar to the one proposed by Ahlrichs *et al.* as a universal form for closed shell systems,[20]

$$\phi(r) = \exp(\alpha - \beta r - \gamma r^2) - \left(\frac{C_6}{r_6} + \frac{C_8}{r_8} + \frac{C_{10}}{r_{10}}\right) \times \exp\left[-\left(\frac{r_m}{r} - 1\right)^2\right], \quad (1)$$

which has been successfully applied to model $H_2$-$H_2$ interaction,[10] and shall be called exp-6-8-10 potential hereafter. The last potential considered is the Buckingham exp-6 LJ form of the 12-6 LJ potential (labeled as exp-6 LJ),

$$\phi(r) = A\ \exp(-\lambda r) - \frac{B}{r_6}, \quad (2)$$

which has also been recently used in the study of hydrogen storage.[15] In all these formula, $r$ refers to the distance between $H_2$ and a carbon atom. The formula is fitted by the generalized-simulated-annealing method.[21]

Two sets of *ab initio* data are used as target values. The first is the $H_2$-coronenen PES obtained by Ferre-Vilaplana at the MP2/aug-cc-pVTZ level, which will be referred to as the FV curve.[13] As $H_2$ is positioned above the center of the seven aromatic rings in coronene, its interactions with the 12 hydrogen atoms at the edge of coronene are negligible, and thus taken as zero. The interaction between a $H_2$ and an infinite graphene can be modeled by further increasing the size of the PAH so that the edge carbon atoms are beyond the cutoff distance for van der Waals interaction. In this case, the adsorption energy of 0.075 eV, extrapolated from the *ab initio* results by Heine and co-workers, are used as the target value.[14] Such an adsorption energy is slightly higher than the experimentally determined value of 0.051 eV which was measured at 100 K and underestimated due to temperature effects.[19]

### B. First principles calculations

To further compare the trend in the repulsive part of the PES, additional *ab initio* calculations are performed, with the GAUSSIAN 03 package.[22] The graphene is modeled by a coronene molecule. The methods for the electronic calculation include both MP2 and DFT with various functionals. The basis set is 6-31G for geometry optimization and aug-cc-pvdz for the calculation of single point energy, which is further corrected by BSSE. To save computational cost, the qualities of such basis sets are not as good as those in previous reports. Our limited purpose for these calculations is to compare the trends in the repulsive region, rather than to reproduce the well-studied equilibrium region.

### C. Confinement of $H_2$ in graphite

The free energy change for trapping $H_2$ between graphite layers, as suggested in a previous LDA study,[8] is reexamined using the empirical PES obtained. The change is defined by the free energy difference between the sandwiched structure with one $H_2$ trapped by two hexagonal rings,[8] and the free $H_2$ gas plus pure graphite. Graphite is modeled by stacking up graphene sheets, each of which is a two-dimensional extension of hexagonal carbon rings, in a periodic unit cell of 29.5 Å × 25.5 Å × 32.3 Å with 2880 atoms. The simulation cell for pure $H_2$ gas contains 2400 molecules. For the intercalated system, the initial structure is built by enlarging the layer spacing between adjacent graphite layers and setting one $H_2$ molecule above each hexagonal ring. The simulation cell is about 29.7 Å × 25.7 Å × 29.4 Å in size and contains 720 $H_2$ molecules and 1440 carbon atoms.

In present calculations, the energy and volume of $H_2$ are obtained by canonical molecular dynamics (MD) simulations at 200 K, in which temperature is controlled by a Nosé-Hoover thermostat.[23,24] The entropy of $H_2$ is taken from experimental value.[25] The volume and energy change of pure graphite and $H_2$ intercalated graphite under external pressure are calculated at 0 K using standard constant pressure MD techniques.[26–28] The periodical boundary condition is used in all current simulations.

The interaction between $H_2$ is modeled by the Silvera-Goldman potential,[29] widely used in many studies.[10] The cutoff for $H_2$ is 12 Å. The Tersoff-type many-body potential[30] with the parameters given by Brenner[31] is used for the covalent interactions between carbon atoms. This potential has been widely applied to simulate diamond, graphite, carbon nanotubes and many hydrocarbon complexes.[32–37] The inter-

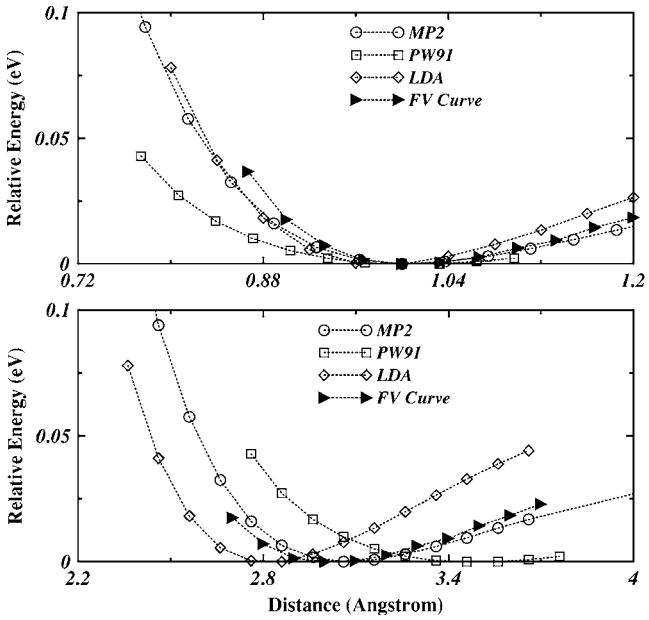


FIG. 1. The *ab initio* PES for the interaction between $H_2$ and coronene. In both panels, the minimum energy is set at zero for all curves, while in the upper panel, the $x$ axis is the ratio between the $H_2$-graphite distance and the equilibrium distance. For the DFT based calculations (LDA and PW91), the basis set is 6-31G, while for the MP2 calculation, the basis set is aug-cc-pvdz.

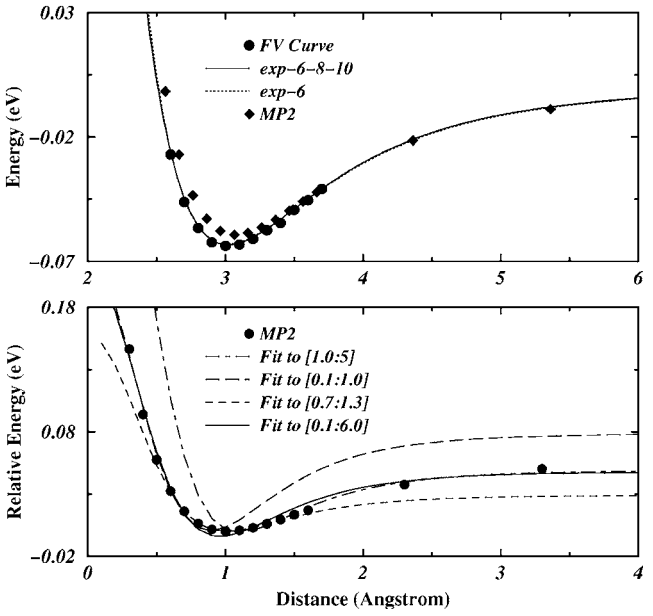


FIG. 2. Fitting of the FV curve. Upper panel, the fitted exp-6-8-10 and exp-6 LJ PES, in comparison with the FV and the MP2/aug-cc-pvdz curves. Lower panel, the fitted 12-6 LJ curve, in comparison with the MP2/aug-cc-pvdz curve, with the brackets specifying the data range of the fitting. For example, [1.0:5.0] indicates that the data points between 1.0 Å to 5.0 Å are used in the fitting. Also in the lower panel, the equilibrium distance is artificially shifted to 1 Å, and the energy is relative to the minimum.

layer van der Waals interaction between two carbon atoms are modeled by the LJ potential, $V_{\mathrm{vdW}}=C_{12}/r^{12}-C_6/r^6$, where $C_6=20$ eV Å$^6$ and $C_{12}=2.48\times10^4$ eV Å$^{12}$.[38] This approach has been successfully used to describe the mechanical properties and the phase transition of isolated DWCNT.[39] The cutoff of 12-6 LJ potential is set as 12 Å.

## III. RESULTS AND DISCUSSIONS

### A. Comparison among *ab initio* results in the repulsive region

Many comparisons have already been made for the $H_2$-coronene interaction curve among various first principles methods around the equilibrium region.[13,14,16] For the compression of $H_2$, the equilibrium distance and the slope in the repulsive part of the potential are more important than the adsorption energy. For that purpose, the PES obtained by a number of *ab initio* calculations are shown in the lower panel of Fig. 1, together with the FV curve, with the minimum energy for each curve set to zero. As expected, only the MP2/aug-cc-pvdz curve reproduces equilibrium distance between $H_2$ and graphene, while LDA significantly underestimates the distance, and both PW91 and B3LYP overestimate it.

More illustrative is the upper panel of Fig. 1, in which the $x$ axis is the ratio between $H_2$-graphite distance and the equilibrium distance, to highlight the difference in the repulsive part of the PES. The repulsion part in the PW91 curves is considerably softer than that in the FV curve, and the same is true for the B3LYP curve not shown in the figure. The gradient corrected functionals thus produce a shallow adsorption well, and at the same time, a less repulsive potential below the equilibrium distance. On the other hand, the LDA curve is in reasonable agreement with the FV curve in the repulsive region and only slightly stiffer, despite the fact that $H_2$ is overbound on graphene according to LDA results. It is clear from such comparisons that the gradient corrected functionals are not suitable for the study in high pressure. However, whether the LDA functional is adequate remains an open question. As for the comparison between MP2/aug-cc-pvdz and the FV curves, the agreement between the two is quite good.

### B. Potential fitting

Both the exp-6-8-10 and exp-6 LJ formula produce excellent fit to the FV curve, for both the equilibrium and the repulsive regions, as shown in the top panel of Fig. 2. The parameters are shown in Table I, while the equilibrium distance and adsorption energy are shown in Table II. The MP2/aug-cc-pvdz curve is again shown along side the FV curve. Although it differs slightly from the FV curve in the equilibrium region due to the smaller basis set, there is good agreement between the two in the repulsive region.

In contrast, it is difficult to fit the 12-6 LJ potential to the *ab initio* calculated PES, be it either the FV curve or the MP2/aug-cc-pvdz curve, although such a potential has been employed in a number of previous studies on the interaction between hydrogen and carbon materials.[40–44] As illustrated in the lower panel of Fig. 2 by the fitting for the MP2/aug-cc-pvdz curve, the PES reproduces the repulsive part reasonably, when all the data points of the MP2/aug-cc-pvdz results

TABLE I. Fitted parameters for exp-6-8-10, exp-6 LJ, and 12-6 LJ potentials.

| exp-6-8-10 | | | | | | |
|---|---|---|---|---|---|---|
| $\alpha$ | $\beta$ (Å$^{-1}$) | $\gamma$ (Å$^{-2}$) | $C_6$ (Å$^6$) | $C_8$ (Å$^8$) | $C_{10}$ (Å$^{10}$) | $r_m$ (Å) |
| 1.55888 | 0.0 | 0.642395 | 15.978 | 0.0 | 1166.92 | 6.21452 |
| exp-6 LJ | | | | | | |
| | | $A$ (eV) | $\lambda$ (Å$^{-1}$) | $B$ (eV Å$^6$) | | |
| | | 1059.13 | 3.54693 | 17.417 | | |
| 12-6 LJ | | | | | | |
| | | $\sigma$ (Å) | | $\varepsilon$ (eV) | | |
| | | 3.02463 | | 0.0221406 | | |

are used. Unfortunately, the fit in the equilibrium and long range regions is far from satisfactory. This fit is labeled as [0.1:6.0] to indicate the range of distance for the data points from 0.1 to 6.0 Å, in which the equilibrium distance is artificially moved to 1 Å and the minimum energy to zero for better comparison. When the fitting is made to the long range part, a much stiff repulsion is obtained (e.g., dash-dotted line, [1.0:5.0]). On the other hand, a good fit to the short range part produces too deep an adsorption well (long-dashed line, [0.1:1.0]). And finally, when the fit is focused on the part near the minimum, the absorption well is too shallow (short-dashed line, [0.7:1.3]). Similar problems are encountered while fitting all the other *ab initio* PES. For the interaction between two hydrogen molecules, it has been well known that LJ potential is inadequate.[10] The same is true for the $H_2$-graphite interaction, and the LJ potential is inadequate to describe the full range *ab initio* results covering both the attractive and the repulsive regions.

In Table II, the equilibrium distance and adsorption energy for the $H_2$-coronene and $H_2$-graphene systems are compared among the exp-6-8-10, exp-6 LJ, and 12-6 LJ PES, as well as with the *ab initio* results and the 12-6 LJ PES reported before.[40–42] Again, the best fit is only achieved by the exp-6-8-10 and exp-6 LJ PES, with the former slightly better than the latter. Thus for isotropic interactions, both exp-6-8-10 and exp-6 LJ potentials as listed in Table I should provide excellent description for the interaction between $H_2$ and graphitic materials, over both the long range attraction and the short range repulsion. It is interesting to notice that the simple formula exp-6 LJ is already sufficient for a good fit to the *ab initio* results, in which the $R^{-6}$ part obviously describes the long range interaction, and the exponential part describes the short range. The exp-6-8-10 is a slightly better fit than exp-6 LJ, although the formula is considerably more complex.

### C. Reexamination on the confinement of $H_2$ in graphite

In a recent LDA study, it was suggested that hydrogen molecules could be confined between two graphene layers at high pressure by sandwiching one $H_2$ between two hexagonal carbon rings.[8] With the new exp-6-8-10 potential, this problem is now reexamined, with the computational details presented in the preceding section. For better comparison, our calculated energetic values are scaled to the periodic cell previously used by Chan *et al.* which contains two graphene layers with 16 carbon atoms and eight $H_2$ molecules.[8] For such a system, the free energy change for the process from pure graphite and $H_2$ to the sandwich structure is calculated by

$$\begin{aligned}\Delta G &= \Delta E + p\Delta V - T\Delta S \\ &= E_S - (E_G + 8E_{H_2}) + p[V_s - (V_G + 8V_{H_2})] \\ &\quad - T[S_S - (S_G + 8S_{H_2})],\end{aligned} \tag{3}$$

where $E$ is the energy, $p$ the pressure, $V$ the volume, $T$ the

TABLE II. Interaction of $H_2$ with coronene and graphene, with $d$ being the equilibrium distance and $E$ being the adsorption energy.

| | 12-6 LJ Ref. 40 | 12-6 LJ Ref. 41 | 12-6 LJ Ref. 42 | 12-6 LJ This study | exp-6 LJ | exp-6-8-10 | *Ab initio* Refs. 13 and 14 |
|---|---|---|---|---|---|---|---|
| | | | | $H_2$ on coronene | | | |
| $d$ (Å) | 3.15 | 3.21 | 2.91 | 2.97 | 3.01 | 3.02 | 3.0 |
| $E$ (eV) | 0.0342 | 0.035 | 0.0423 | 0.0648 | 0.0632 | 0.0634 | 0.064 |
| | | | | $H_2$ on graphene | | | |
| $d$ (Å) | 3.13 | 3.18 | 2.90 | 2.96 | 2.99 | 3.00 | 3.0 |
| $E$ (eV) | 0.0417 | 0.0431 | 0.0497 | 0.0768 | 0.0755 | 0.0749 | 0.075 |

TABLE III. Thermodynamic quantities as a function of pressure, calculated by exp-6-8-10 potential and the experimental equation of state.

| Pressure (GPa) | $\Delta E$ (eV) | $V_S - V_G$ (Å$^3$) | $8V_{H_2}$ (Å$^3$) | $p\Delta V$ (eV) | $\Delta H$ (eV) $=\Delta E + p\Delta V$ | $-T\Delta S$ (eV) | $\Delta G$ (eV) |
|---|---|---|---|---|---|---|---|
| 0.00 | 0.701 | | | | | | |
| 0.50 | 0.618 | 110.993 | 219.713 | −0.340 | 0.278 | 0.782 | 1.060 |
| 1.00 | 0.548 | 108.039 | 175.565 | −0.422 | 0.126 | 0.685 | 0.811 |
| 1.50 | 0.487 | 105.517 | 157.395 | −0.486 | 0.001 | 0.628 | 0.629 |
| 2.00 | 0.434 | 103.274 | 144.682 | −0.517 | −0.083 | 0.592 | 0.509 |
| 2.50 | 0.387 | 101.301 | 135.013 | −0.526 | −0.139 | 0.476 | 0.337 |
| 3.00 | 0.344 | 99.488 | 127.631 | −0.527 | −0.183 | 0.427 | 0.244 |
| 3.50 | 0.306 | 97.863 | 121.882 | −0.525 | −0.218 | 0.399 | 0.181 |
| 4.00 | 0.270 | 96.288 | 117.279 | −0.524 | −0.254 | 0.380 | 0.126 |
| 4.50 | 0.238 | 94.875 | 113.487 | −0.523 | −0.285 | 0.365 | 0.080 |
| 5.00 | 0.207 | 93.532 | 110.277 | −0.523 | −0.315 | 0.353 | 0.038 |
| 5.50 | 0.178 | 92.275 | 107.493 | −0.523 | −0.344 | 0.343 | −0.001 |
| 6.00 | 0.150 | 91.090 | 105.025 | −0.522 | −0.372 | 0.333 | −0.038 |
| 6.50 | 0.122 | 89.964 | 102.798 | −0.521 | −0.399 | 0.325 | −0.074 |
| 7.00 | 0.093 | 88.884 | 100.766 | −0.519 | −0.426 | 0.318 | −0.109 |
| 7.50 | 0.062 | 87.857 | 98.857 | −0.515 | −0.453 | 0.311 | −0.142 |
| 8.00 | 0.029 | 86.874 | 97.072 | −0.509 | −0.480 | 0.305 | −0.175 |

temperature, and $S$ the entropy. Subscript $S$ labels the sandwich structure, G pure graphite, and $H_2$ the hydrogen molecule.[8]

The results shown in Table III are therefore directly comparable to Table I in Ref. 8. Among the three terms for $\Delta G$, the $-T\Delta S$ term is almost the same since it is calculated from experimental results in both cases.[25] The $p\Delta V$ term is calculated from MD simulation in the current study, and less negative than the previous results, in which the volume of $H_2$, $V_{H_2}$, was obtained from experiment. However, the difference is small, which indicates that $V_{H_2}$ can be calculated to reasonable accuracy from MD simulations. The most significant difference is in the $\Delta E$ term, which measures the energy change for the confinement process. At zero pressure and 200 K, $\Delta E$ is endothermic by 0.70 eV in MD results, compared to a much smaller value of 0.14 eV in the previous LDA results. Further analysis shows that the difference of 0.56 eV is largely due to the repulsion between $H_2$ molecules trapped at the centers of hexagonal rings. The distance between two neighboring $H_2$ molecules is around 2.4 Å, and the repulsive energy is around 0.08 eV according to experiments[10] and well reproduced by the Silvera-Goldman potential[29] employed in the current study. In contrast, the LDA potential for $H_2$-$H_2$ interaction produces too short an equilibrium distance at 2.89 Å, compared to the experimental value around 3.3 Å. As a result, the $H_2$-$H_2$ repulsion at 2.4 Å is just below 0.01 eV and significantly underestimated. With six unique pairs of $H_2$ interactions in the unit cell, such repulsive energy is underestimated by 0.42 eV, which accounts for most of the discrepancy (0.56 eV). Although the shape of the repulsive part of the LDA potential is in reasonable agreement with the *ab initio* results, as indicated in Fig. 1 for the $H_2$-coronene interaction, the equilibrium distance does have a significant impact for the simulation of high density states. The underestimate for the $H_2$-$H_2$ repulsive energy in LDA results is directly responsible for a significant underestimate of the endothermic energy change for the confinement of $H_2$ between graphite.

With a larger $\Delta E$, the Gibbs free energy change for $H_2$ confinement is more difficult than previously estimated by LDA. However, as the pressure increases, $\Delta E$ decreases as the $H_2$-graphene repulsion in the sandwich structure increases less than that between graphene layers in graphite, similar to the trend observed in LDA calculations.[8] At the same time, $p\Delta V$ becomes more negative with increasing pressure, until it flattens around 2.5 GPa. The $-T\Delta S$ term also becomes less endothermic with pressure, mostly due to the decrease of $S_{H_2}$. Due to these trends as shown in Fig. 3, the $\Delta G$ value falls below zero at 200 K when the external pressure reaches 5.5 GPa which is considerably higher than the threshold of 1.5 GPa based on LDA results.

For structural parameters, the distance between two neighboring graphene layers at zero pressure is increased to 5.88 Å from 3.23 Å for pure graphite, and is considerably larger than the value of 5.432 Å of LDA results.[8] This is again due to the shallower potential well and longer equilibrium $H_2$-graphene distance in the new potential than those in the LDA potential. The insertion of $H_2$ also produces an increase of ~2% in C-C bond distance. Upon application of pressure, the volume of the system decreases mainly due to the shortening of the layer spacing between graphene (~10%), while the C-C bond distance decreases only by ~ 2%, as shown in Fig. 4, in which the C-C bond distance and interlayer spacing are plotted against the pressure.

At GPa pressure, it would be difficult to force $H_2$ between graphene layers in real application, due to kinetic reasons, despite the sign change in $\Delta G$. However, as pointed out

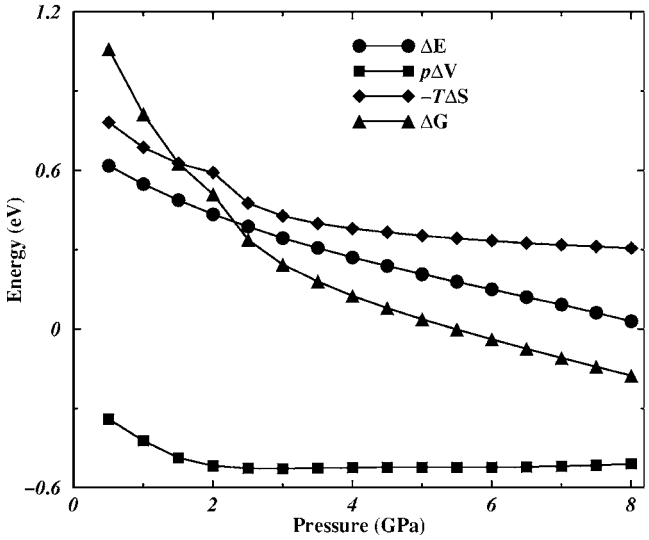


FIG. 3. Thermodynamic data for the trapping process as a function of pressure at 200 K, estimated by molecular-dynamics calculation using the exp-6-8-10 potential and experimental equation of state for $H_2$.

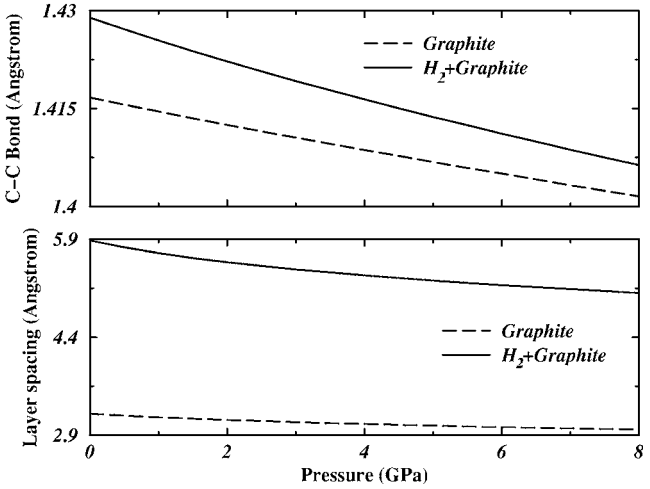


FIG. 4. The C-C bond length (upper panel) and layer spacing between neighboring graphene sheet (lower panel) as a function of pressure for both pure graphite (dashed line) and $H_2$ intercalated graphite (solid line).

before,[8] the graphene layers can be expanded by intercalation.[45] In that case, the volume difference $V_s - V_g$ would be reduced to almost zero, and correspondingly the $p\Delta V$ term is determined simply by $-8pV_{H_2}$. Using the numbers presented in Table III and assuming little change in $\Delta E$, it is roughly estimated that trapping $H_2$ between the hexagonal rings can then be achieved below 1.5 GPa at 200 K. It should also be pointed out that a precise description of the motion of $H_2$ molecule usually requires quantum treatment. However the thermodynamic behavior of free $H_2$ gas around 200 K is essentially classical. Accounting for the weak trapping potential, the quantum correction could change the numbers slightly, but not the main conclusion in the above analysis.

## IV. CONCLUSION

The recent high level *ab initio* results on the interaction between $H_2$ and graphite as modeled by a coronene molecule cannot be easily fit to a LJ potential, while both exp-6-8-10 and exp-6 LJ potentials can describe both the long range attractive and short range repulsive regions. Such potentials should be useful in the future studies on the interaction between $H_2$ and graphitic materials, both in the physisorption and the high density–high pressure regimes. A reexamination on the trapping of $H_2$ in graphite at high pressure, using the new exp-6-8-10 potential, indicates that the critical pressure is considerably higher than that previous obtained by LDA calculation, because the equilibrium distance between two $H_2$ molecules is underestimated by LDA and therefore the repulsive energy between $H_2$ molecules in the trapped state is also underestimated.

## ACKNOWLEDGMENTS

The authors thank A. Ferre-Vilaplana for providing us the data presented in Ref. 13. The work reported is partially supported by an Earmarked Grant (Contract No. CUHK 4023/05P) from the Research Council of Hong Kong SAR Government. Two of the authors (D.Y.S. and X.G.G.) acknowledge support from the National Science Foundation of China. One of the authors (D.Y.S.) also thanks Shanghai Municipal Education Commission and Shanghai Education Development Foundation (Shuguang Project and Shanghai Pujiang Project). The authors are grateful for the generous allocation of computer time on the computer clusters at the Chemistry Department, and the Center for Scientific Modeling and Computation, and on the high performance computing facilities at the Information Technology Service Center, all located at The Chinese University of Hong Kong.

*Electronic address: zfliu@cuhk.edu.hk

[1] L. Schlapbach and A. Zuttel, Nature (London) **414**, 353 (2001).
[2] M. S. Dresselhaus, K. A. Williams, and P. C. Eklund, MRS Bull. **24**, 45 (1999).
[3] A. C. Dillon and M. J. Heben, Appl. Phys. A: Mater. Sci. Process. **72**, 133 (2001).
[4] A. Zuttel, P. Sudan, P. Mauron, and P. Wenger, Appl. Phys. A: Mater. Sci. Process. **78**, 941 (2004).
[5] P. Sudan *et al.*, Carbon **41**, 2377 (2003).
[6] W. L. Mao and H. K. Mao, Proc. Natl. Acad. Sci. U.S.A. **101**, 708 (2004).
[7] S. P. Chan, G. Chen, X. G. Gong, and Z. F. Liu, Phys. Rev. Lett. **87**, 205502 (2001).
[8] S. P. Chan, M. Ji, X. G. Gong, and Z. F. Liu, Phys. Rev. B **69**,

092101 (2004).
[9] A. W. C. van den Berg, S. T. Bromley, J. C. Wojdel, and J. C. Jansen, Phys. Rev. B **72**, 155428 (2005).
[10] I. F. Silvera, Rev. Mod. Phys. **52**, 393 (1980).
[11] H. K. Mao and R. J. Hemley, Rev. Mod. Phys. **66**, 671 (1994).
[12] J. S. Arellano, L. M. Molina, A. Rubio, and J. A. Alonso, J. Chem. Phys. **112**, 8114 (2000).
[13] A. Ferre-Vilaplana, J. Chem. Phys. **122**, 104709 (2005).
[14] T. Heine, L. Zhechkov, and G. Seifert, Phys. Chem. Chem. Phys. **6**, 980 (2004).
[15] S. Patchkovskii *et al.*, Proc. Natl. Acad. Sci. U.S.A. **102**, 10439 (2005).
[16] F. Tran *et al.*, J. Phys. Chem. B **106**, 8689 (2002).
[17] Y. Okamoto and Y. Miyamoto, J. Phys. Chem. B **105**, 3470 (2001).
[18] Y. K. Zhang, W. Pan, and W. T. Yang, J. Chem. Phys. **107**, 7921 (1997).
[19] L. Mattera *et al.*, Surf. Sci. **93**, 515 (1980).
[20] R. Ahlrichs, R. Penco, and G. Scoles, Chem. Phys. **19**, 119 (1977).
[21] Y. Xiang, D. Y. Sun, W. Fan, and X. G. Gong, Phys. Lett. A **233**, 216 (1997).
[22] M. J. Frisch *et al.*, GAUSSIAN 03, Revision A.1 (Gaussian, Inc., Pittsburgh, PA, 2003).
[23] S. Nosé, J. Chem. Phys. **81**, 511 (1984).
[24] W. G. Hoover, Phys. Rev. A **31**, 1695 (1985).
[25] H. Hemmes, A. Driessen, and R. Griessen, J. Phys. C **19**, 3571 (1986).
[26] M. Parrinello and A. Rahman, J. Appl. Phys. **52**, 7182 (1981).
[27] M. Parrinello and A. Rahman, Phys. Rev. Lett. **45**, 1196 (1980).
[28] H. C. Andersen, J. Chem. Phys. **72**, 2384 (1980).
[29] I. F. Silvera and V. V. Goldman, J. Chem. Phys. **69**, 4209 (1978).
[30] J. Tersoff, Phys. Rev. Lett. **61**, 2879 (1988).
[31] D. W. Brenner, Phys. Rev. B **42**, 9458 (1990).
[32] D. H. Robertson, D. W. Brenner, and J. W. Mintmire, Phys. Rev. B **45**, 12592 (1992).
[33] B. I. Yakobson, C. J. Brabec, and J. Bernholc, Phys. Rev. Lett. **76**, 2511 (1996).
[34] M. B. Nardelli, B. I. Yakobson, and J. Bernholc, Phys. Rev. Lett. **81**, 4656 (1998).
[35] Y. Y. Xia *et al.*, Phys. Rev. B **61**, 11088 (2000).
[36] A. N. Kolmogorov and V. H. Crespi, Phys. Rev. Lett. **85**, 4727 (2000).
[37] Y. C. Ma, Y. Y. Xia, M. W. Zhao, R. J. Wang, and L. M. Mei, Phys. Rev. B **63**, 115422 (2001).
[38] L. Henrard, E. Hernandez, P. Bernier, and A. Rubio, Phys. Rev. B **60**, R8521 (1999).
[39] X. Ye, D. Y. Sun, and X. G. Gong, Phys. Rev. B **72**, 035454 (2005).
[40] G. Stan, M. J. Bojan, S. Curtarolo, S. M. Gatica, and M. W. Cole, Phys. Rev. B **62**, 2173 (2000).
[41] S. C. Wang, L. Senbetu, and C. W. Woo, J. Low Temp. Phys. **41**, 611 (1980).
[42] K. A. Williams, B. K. Pradhan, P. C. Eklund, M. K. Kostov, and M. W. Cole, Phys. Rev. Lett. **88**, 165502 (2002).
[43] D. Levesque, A. Gicquel, F. L. Darkrim, and S. B. Kayiran, J. Phys.: Condens. Matter **14**, 9285 (2002).
[44] F. Darkrim and D. Levesque, J. Chem. Phys. **109**, 4981 (1998).
[45] M. S. Dresselhaus and G. Dresselhaus, Adv. Phys. **30**, 139 (1981).